Human Molecular Genetics, 2009, Vol. 18, No. 9 **1633–1641**
doi:10.1093/hmg/ddp081
Advance Access published on March 2, 2009

Heterozygous mutations of the voltage-gated sodium channel *SCN8A* are associated with spike-wave discharges and absence epilepsy in mice

Ligia A. Papale[1,2,†], Barbara Beyer[3,†], Julie M. Jones[4], Lisa M. Sharkey[4], Sergio Tufik[2], Michael Epstein[1], Verity A. Letts[3], Miriam H. Meisler[4], Wayne N. Frankel[3,*] and Andrew Escayg[1]

[1]Department of Human Genetics, Emory University, Atlanta, GA 30322, USA, [2]Department of Psychobiology, Universidade Federal de São Paulo, São Paulo, Brazil, [3]The Jackson Laboratory, 600 Main Street, Bar Harbor, ME 04609, USA and [4]Department of Human Genetics, University of Michigan, Ann Arbor, MI 48109-5618, USA

Received January 9, 2009; Revised and Accepted February 16, 2009

In a chemical mutagenesis screen, we identified the novel *Scn8a^{8J}* allele of the gene encoding the neuronal voltage-gated sodium channel $Na_v1.6$. The missense mutation V929F in this allele alters an evolutionarily conserved residue in the pore loop of domain 2 of $Na_v1.6$. Electroencephalography (EEG) revealed well-defined spike-wave discharges (SWD), the hallmark of absence epilepsy, in *Scn8a^{8J}* heterozygotes and in heterozygotes for two classical *Scn8a* alleles, *Scn8a^{med}* (null) and *Scn8a$^{med\text{-}jo}$* (missense). Mouse strain background had a significant effect on SWD, with mutants on the C3HeB/FeJ strain showing a higher incidence than on C57BL/6J. The abnormal EEG patterns in heterozygous mutant mice and the influence of genetic background on SWD make *SCN8A* an attractive candidate gene for common human absence epilepsy, a genetically complex disorder.

INTRODUCTION

The voltage-gated sodium channels include four genes with high expression levels in neurons of the central nervous system: *SCN1A*, which encodes $Na_v1.1$, *SCN2A* encoding $Na_v1.2$, *SCN3A* encoding $Na_v1.3$ and *SCN8A* encoding $Na_v1.6$. Voltage-gated sodium channels are responsible for initiation and propagation of transient depolarizing currents and play an important role in electrical signaling between cells. In patients with epilepsy, >300 mutations in *SCN1A* have been identified, the vast majority of which are *de novo* mutations in children with severe myoclonic epilepsy of infancy (1,2). A small number of mutations have been identified in *SCN2A* and *SCN3A* in other inherited epilepsies (1,3). Structure/function relationships of the mutated sodium channels remain unclear, and most of the mutations seem to affect multiple biophysical parameters. One frequent feature of pathogenic missense mutations is an increase in persistent sodium current that may facilitate premature and sustained firing.

To date, 13 mutant alleles of mouse *Scn8a* have been described, including seven spontaneous and four *N*-ethyl-*N*-nitrosourea (ENU)-induced alleles (4). Electrophysiological analyses of *Scn8a* mutant mice have revealed several unique features of $Na_v1.6$ mediated sodium currents. This channel is responsible for an unusual conductance termed the resurgent current that flows during repolarization, and also contributes to persistent and subthreshold sodium currents in various types of neurons (5–9). $Na_v1.6$ is localized to the axon initial segment and it is the major sodium channel at the nodes of Ranvier in adult myelinated axons (10,11).

Mice with *Scn8a* mutations often exhibit ataxic gait, consistent with the critical role of $Na_v1.6$ in the repetitive firing of Purkinje cells. Tremor and loss of hind limb function are also common in homozygous *Scn8a* mutants, and null homozygotes do not survive beyond 3 weeks of age. Conditional inactivation of a floxed allele of *Scn8a* in both cerebellar Purkinje and granule cells is sufficient to produce ataxic gait and tremor, demonstrating the critical role of cerebellar $Na_v1.6$ in normal locomotion (12). Although heterozygous mice with

*To whom correspondence should be addressed. Tel: +1 2072886354; Fax: +1 2072886757; Email: wayne.frankel@jax.org
†The first two authors contributed equally to the study.

null mutations are not ataxic, they do exhibit subtle behavioral deficits (13). Furthermore, heterozygous patients in a human family segregating a null allele of *SCN8A* exhibited cognitive and behavioral deficits (14).

Absence epilepsy is a non-convulsive form of idiopathic generalized epilepsy that is characterized by recurrent seizures in patients without brain lesions. It often occurs in childhood and adolescence, with a prevalence of ~10% among children with any type of epilepsy. Typical absence seizures are associated with 3–4 Hz spike-wave discharges (SWD) on the electroencephalogram (EEG) and are characterized by a brief loss of consciousness of abrupt onset and termination coincident with SWD. Although the general clinical features of absence seizures have been known for decades and a genetic etiology is suspected, a full understanding of the genetic basis of absence epilepsy, and molecular and cellular mechanisms have been elusive.

There are now several rodent models of absence epilepsy with genetic etiology, including polygenic models such as the WAG/Rij (15) and GAERS (16) rat strains and the inbred mouse strain A/J (17). The inbred mouse strain C3H/HeJ carries a mutation in *Gria4*, encoding an AMPA receptor subunit, which has a major effect on the generation of absence seizures (18). Mutations in each of the four major subunits of voltage-gated Ca^{2+} channels (19–22) and the knockout of *Hcn2* encoding an I_h channel (23) have provided monogenic mouse models of recessively inherited absence epilepsy. The knockout of *Cacna1g*, encoding a T-type Ca^{2+} channel subunit, confers resistance to chemically and genetically induced absence seizures (24), consistent with the observation that dominant mutations in human *CACNA1G* can lead to absence epilepsy (25). A mutation in a splice variant of the T-type calcium channel gene *Cacna1h* has also been shown to contribute to the absence epilepsy phenotype in the GAERS rat model (26). These results underscore the central role of T-type Ca^{2+} channels in generating the normal thalamocortical oscillations that become impaired during absence seizures.

Absence seizures are also observed in a knock-in mouse model with the human R43Q point mutation in *GABRG2*, encoding a $GABA_A$ receptor subunit, which was identified in a family with a spectrum of generalized seizure phenotypes (27,28). Until now, the *Gabrg2* R43Q knock-in mouse had been the only model of dominantly inherited absence epilepsy reported. Here we describe dominantly inherited absence epilepsy associated with three alleles of the sodium channel *Scn8a* and demonstrate that the severity of the phenotype is influenced by genetic background, making *SCN8A* an intriguing candidate gene for human absence epilepsy.

RESULTS

Origin of *Scn8a*^{8J}

The new allele of *Scn8a* was initially detected in neurologically impaired animals from a standard three-generation ENU mutagenesis screen for recessive mutations carried out in the ReproGenomics facility at Jackson Laboratory. C57BL/6J (B6) mice were mutagenized and subsequently crossed to strain C3HeB/FeJ (FeJ) to generate potentially homozygous G_3 animals (see http://reproductivegenomics.jax.org). In pedigree 596-16, 16 of 38 G_3 mice were smaller than wild-type littermates and had impaired locomotor function with a weak and unsteady gait. Since neither parent was affected, the trait was presumed to be recessive. Homozygous mutants usually did not survive past 21 days, although a few survived as long as 7 weeks when left with the dams and fed with ground rather than solid grain pellets.

Genetic mapping and identification of the ENU-induced mutation in *Scn8a*

The recessive locomotor trait was mapped to telomeric chromosome 15 in a genome scan of 73 G_3 and G_3F_1 mice including both affected and unaffected individuals (Fig. 1A). A survey of candidate genes located within the linked region identified the *Scn8a* gene at 100.7 Mb (Fig. 1A). Mutations of *Scn8a* are known to produce locomotor abnormalities (4). To determine whether line 596-16 carried a new allele of *Scn8a*, we carried out a complementation test by crossing unaffected carriers from line 596-16 with heterozygotes for the *med* allele of *Scn8a*, a null mutant (29). Among six litters with 38 offspring from the complementation cross, eight mice exhibited locomotor impairment at 3 weeks of age that was similar to the parental homozygous mice. This observed non-complementation is consistent with allelism of the new mutant with *Scn8a*.

Identification of the *Scn8a* mutation

The 28 exons of *Scn8a* were amplified from affected mice and sequenced. We detected the mutation c.2785G>T in exon 13, which is predicted to change the amino acid valine 929 to phenylalanine (p.V929F) (Fig. 1B). Valine residue 929 is conserved in the vertebrate orthologs of *Scn8a* and in the neuronal paralogs *Scn1a*, *Scn2a* and *Scn3a* (Fig. 1C). This chemically non-conservative substitution is located in the pore region of domain 2 (Fig. 1D). Mutations in the pore regions of the sodium channel are frequently pathogenic in mouse and humans (30). Western blot analysis of brain membrane proteins demonstrated that $Na_v1.6$ protein is present at normal levels in *Scn8a*^{8J} homozygotes (Fig. 1E), suggesting that the V929F substitution may alter channel function.

SWD in *Scn8a*^{8J} mutant mice

SWD were initially observed in two affected homozygous *Scn8a*^{8J} mice from the G_3 generation. Each had a very high incidence of SWD, with a burst frequency of 4–5 Hz (Supplementary Material, Fig. S1). *Scn8a*^{8J} heterozygotes also exhibited prevalent SWD, with a burst frequency of 7–9 Hz, which is more typical of rodent models of absence epilepsy. The SWD were robust, with high amplitude, significant duration and high frequency, and were observed in most or all recording channels (Fig. 2A). SWD usually occurred between periods of locomotor activity. During episodes of SWD mice were immobile except for occasional whisker twitching, as ascertained in real-time and by video-EEG. Although the C3HeB/FeJ strain has a low incidence of SWD (18,31), in the present crosses there was a highly significant difference in the incidence of SWD between *Scn8a*^{8J} hetero-

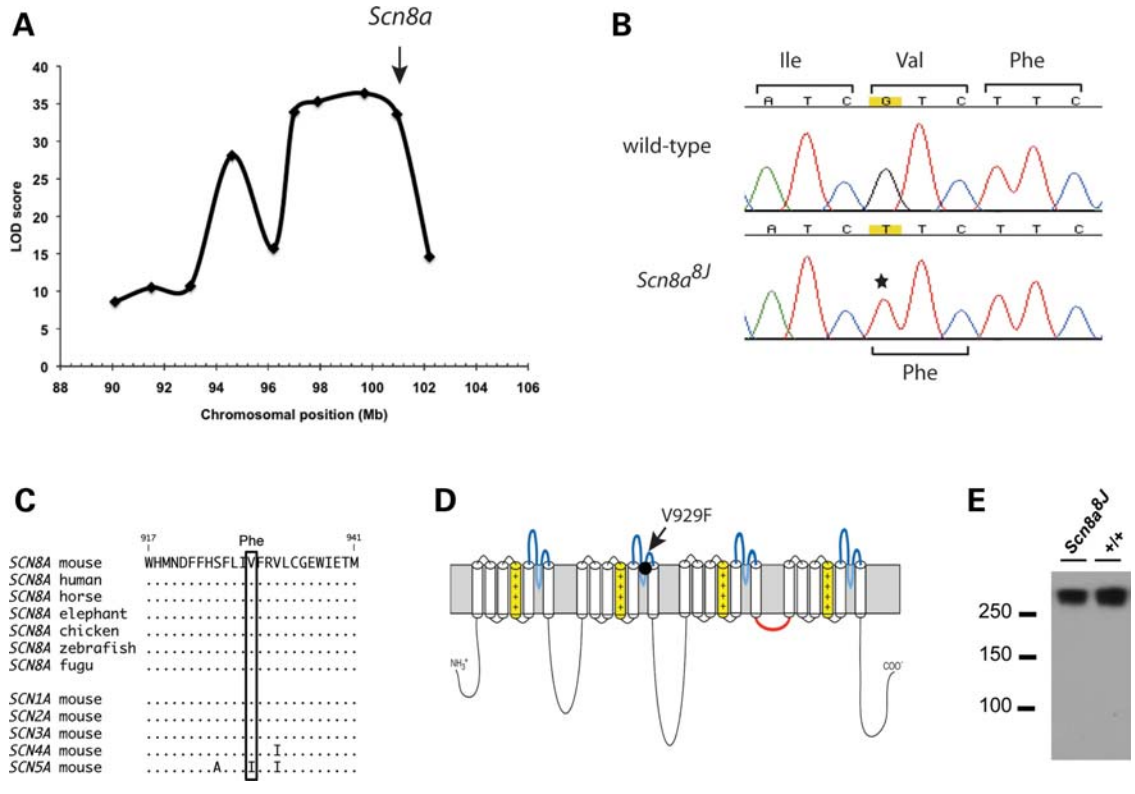

Figure 1. Genetic mapping and identification of the *Scn8a*^{8J} mutation. (**A**) LOD score plot of locomotor impairment in mice from G_3 and G_3F_1 populations. The markers from left to right are *D15Mit171* (90.1 Mb), *D15Mit243* (93.1 Mb), *D15Jmp29* (96.2 Mb), *D15Mit161* (97.0 Mb), *D15Mit43* (97.9 Mb), *D15Mit14* (99.7 Mb), *D15Mit246* (102.1 Mb) and *D15Mit79* (103.4 Mb). *Scn8a* is located at 100.7 Mb (arrow). The maximum LOD score was 36.4 at 99.7 Mb. (**B**) Identification of the mutation (G>T) in a homozygote from the 596-16 pedigree. (**C**) Evolutionary conservation of residue valine 929 in eight vertebrate orthologs and five mouse paralogs of *Scn8a*. (**D**) Location of V929 in the ion pore region of domain 2. (**E**) Western blot of membrane protein from mutant and wild-type mouse brain. Lanes contained 75 μg of protein.

zygotes and their wild-type littermates, indicating a major gene effect of *Scn8a*^{8J} (Fig. 3, $G_3\times$ C3HeB/FeJ; $P = 7.0 \times 10^{-5}$). The high incidence of SWD was retained after heterozygotes were backcrossed to strain C3HeB/FeJ for two more generations (Fig. 3, G_3N_2 and G_3N_3).

SWD in two additional *Scn8a* mutants

To determine whether the SWD in *Scn8a*^{8J} heterozygotes was also present in other *Scn8a* mutants, we examined two classical alleles of *Scn8a*. *Scn8a*^{med} is a loss-of-function allele (29), and *Scn8a*$^{med\text{-}jo}$ is a missense mutation that alters the voltage dependence of activation and inactivation (32). At Emory University, we examined 12 h (7 am to 7 pm) of continuous EEG data from six heterozygotes for *Scn8a*$^{med/+}$ and *Scn8a*$^{med\text{-}jo/+}$. Both alleles conferred high-amplitude SWD of variable duration accompanied by behavior arrest (Fig. 2B and C). The average number of SWD was significantly higher in the *Scn8a*$^{med/+}$ mice compared with wild-type littermates (*Scn8a*$^{med/+}$, 156 ± 28.7 SE ($n = 6$); wild-type, 31.8 ± 5.7 SE ($n = 6$), $P = 0.002$). However, the average incidence of SWD in *Scn8a*$^{med\text{-}jo/+}$ mutants was significantly lower than in *Scn8a*$^{med/+}$ mice (*Scn8a*$^{med\text{-}jo/+}$, 20.7 ± 5.7 SE ($n = 6$), $P = 0.0006$), and we observed no SWD in their wild-type littermates. Because the two laboratories performing EEG analysis use electrode preparations with different sensitivities, it was difficult to directly compare the SWD incidence caused by the *Scn8a*^{8J} allele with that by the two classical *Scn8a* alleles. However, analysis of four C3HeB/FeJ-*Scn8a*$^{med/+}$ mutants at Jackson Laboratory revealed a slightly lower incidence of SWD than that of *Scn8a*^{8J} (Fig. 3, far right; $P = 0.05$).

Reduction in SWD after treatment with ethosuximide

Ethosuximide (ETX) is often the first-line drug for the treatment of absence epilepsy in patients. It is quite selective in its anti-epileptic activity, being ineffective against convulsive and focal seizures. ETX has also been shown to reduce the frequency of SWD in rodent models of absence epilepsy (33). To further characterize the seizure phenotype of the *Scn8a* mutants, we evaluated the effect of acute ETX treatment on the frequency of SWD in heterozygous *Scn8a*^{8J} (Fig. 4A) and *Scn8a*^{med} (Fig. 4B) mutants. The administration of ETX resulted in fewer and shorter SWD episodes in both mutants, consistent with the classification of absence seizures. At Jackson Laboratory, three *Scn8a*$^{8J/+}$ mutants had an average of 85.7 (±5.0 SE) SWD in the 60 min interval prior to ETX administration and 14.7 SWD (±5.8 SE) after ETX, a 6-fold decrease. At Emory, six *Scn8a*$^{med/+}$ mutants averaged 15.1 (±3.96 SE) SWD in the 60 min interval prior to ETX administration and 1.4 (±0.47 SE) SWD in the 60 min after

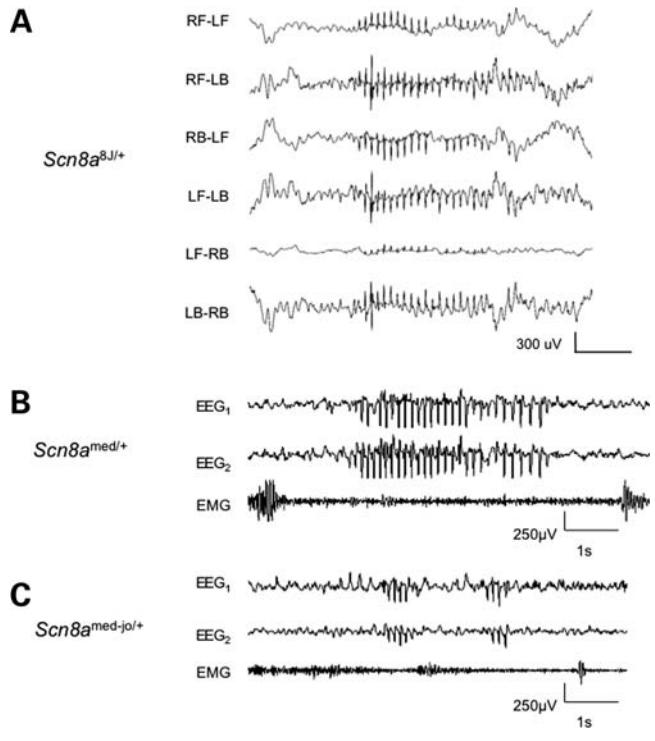

Figure 2. Representative SWD in *Scn8a* mutants. (**A**) Traces correspond to six differential recordings from a $Scn8a^{8J/+}$ mouse from each of four epidural electrodes; RF–LF (right front–left front), RF–LB (right front–left back), etc. carried out at Jackson Laboratory as described in Materials and Methods. SWD data from individual $Scn8a^{8J/+}$ mice is shown in Figure 4. (**B**) and (**C**) Representative EEG traces from $Scn8a^{med/+}$ and $Scn8a^{med\text{-}jo/+}$ mutants, respectively, carried out at Emory University as described in Materials and Methods. EEG_1 and EEG_2 represent cortical activity from the right and left hemispheres, respectively. SWD are present in both hemispheres and are associated with lack of muscle movement.

ETX administration, an 11-fold decrease. To control for the effect of handling, we also determined the frequency of SWD in $Scn8a^{med/+}$ mice after the injection of saline (Fig. 4C). The frequency of SWD in six saline-injected mice increased 3-fold from 13 ($\pm$1.33 SE) SWD in the 60 min interval prior to saline injection to 34.6 ($\pm$10.9 SE) SWD in the 60 min interval after injection, suggesting that the ETX results are a conservative measure of the pharmacological effect.

Genetic background influences the incidence of SWD in $Scn8a^{8J}$ mice

In prior studies, SWD were not detected in the ENU-induced mutation $Scn8a^{nmf58}$, with the amino acid substitution L1404H in the pore region of *Scn8a* domain 3. $Scn8a^{nmf58}$ mice in those studies were generated and tested on the C57BL/6J background (30). In the present study, the fewest SWD were observed in $Scn8a^{med\text{-}jo}$ mice, also on the C57BL/6J background, whereas the other two alleles are on C3HeB/FeJ. To determine whether the C3HeB/FeJ background is an important factor in the incidence of *Scn8a*-associated SWD, we crossed G_3N_3 heterozygous $Scn8a^{8J}$ mice to strain C57BL/6J and tested the F_1 hybrid heterozygotes (~50% C3H-derived) and the first backcross (N_2 generation; ~25% C3H-derived; Fig. 3; G_3N_3, $F_1 \times$ C57BL/6J). The results, showing a linear difference over a 2-fold range between genotypes (Fig. 3 inset), suggest that SWD in $Scn8a^{8J}$ is enhanced by homozygosity for C3HeB/FeJ strain background alleles ($P = 0.001$) and suppressed by homozygosity for B6 alleles ($P = 1.8 \times 10^{-7}$).

Effect of different states of vigilance on the frequency of SWD

A relationship between the incidence of absence seizures and states of vigilance has been noted in humans and animals (34). To examine this relationship in $Scn8a^{med/+}$ mutants, we analyzed 48 h of continuous EEG data and compared the average incidence of SWD in wakefulness, slow-wave sleep (SWS) and paradoxical sleep (PS) during the 12 h dark cycle with the 12 h light cycle. $Scn8a^{med/+}$ mutants showed a similar frequency of SWD during wakefulness in the light and dark cycles (Fig. 5, $P = 0.06$). However, the frequency of SWD during SWS and PS was significantly higher during the dark cycle compared with the corresponding states of vigilance in the light cycle (Fig. 5, $P = 0.03$ for both comparisons).

DISCUSSION

In this study, we show for the first time that heterozygous *Scn8a* mutant mice exhibit the hallmark of absence epilepsy—ETX-sensitive SWD with accompanying brief arrest of normal activity. We observed SWD in mice carrying three alleles: $Scn8a^{8J}$, a new allele with a non-conservative amino acid substitution in the pore region of the channel and the well-characterized mutations $Scn8a^{med}$, a null allele, and $Scn8a^{med\text{-}jo}$, a missense mutation in an intracellular linker that causes altered voltage dependence. Although the functional impact of the $Scn8a^{8J}$ V929F amino acid substitution on Na^+ channel activity is not yet known, the similar SWD phenotype of three different mutant alleles suggests a critical role for *Scn8a* in the regulation of thalamocortical function. We also noted that strain background has a strong effect on the incidence of SWD in $Scn8a^{8J}$ heterozygotes, with a higher incidence on the C3HeB/FeJ strain than on C57BL/6J. Future work will allow the mapping and identification of genetic modifiers that enhance or suppress SWD, which will be of interest for understanding absence epilepsy as a complex genetic trait.

The discovery of absence seizures in *Scn8a* mutants is somewhat surprising, because these mice have been studied for many years. However, systematic EEG analysis of *Scn8a* mutants was not part of the characterization of most of the previously described mutants. Human absence seizures are often overlooked, as well, because of their brevity and lack of post-ictal deficits. The lack of SWD in mice homozygous for the ENU-induced mutation $Scn8a^{nmf58}$ may be explained, in part, by their coisogenic C57BL/6J strain background (30). In the present study, $Scn8a^{8J}$ homozygotes on a predominantly C3HeB/FeJ background were identified during an unrelated phenotype screen, and EEG recording was carried out prior to the identification of the mutated gene. $Scn8a^{8J}$ homozygotes

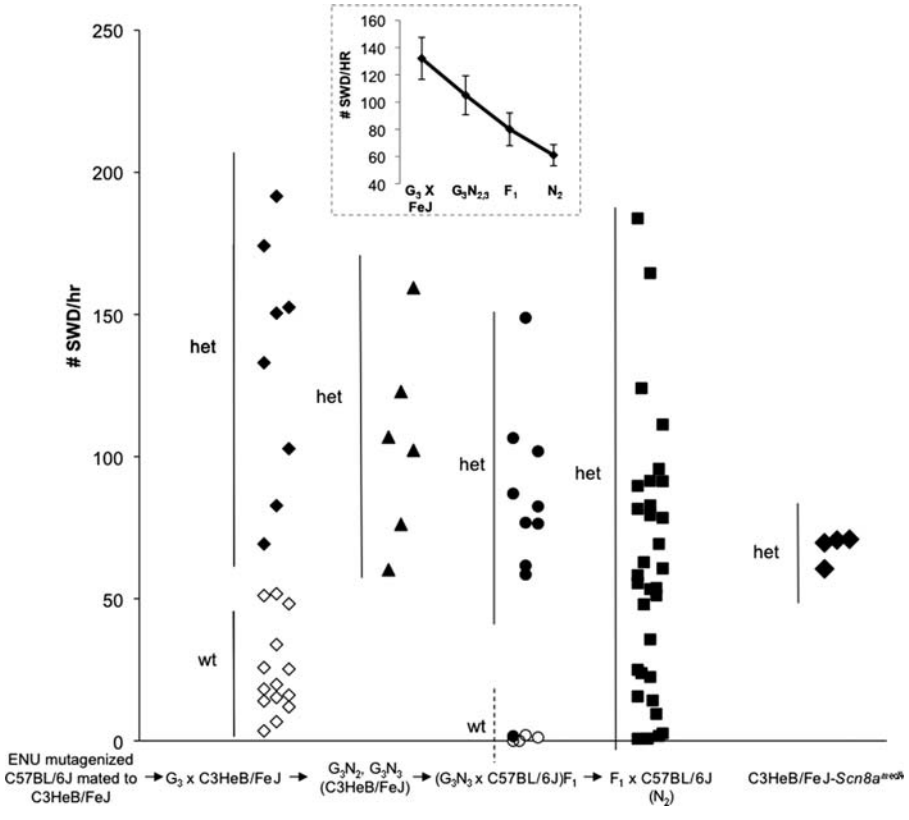

Figure 3. Effect of genetic background on incidence of SWD in heterozygous *Scn8a*^{8J}mice. Each point shows the number of SWD per hour for an individual mouse, in different genetic backgrounds. Heterozygous (het) genotypes are shown in filled symbols, wild-type (wt) in open symbols. The inset shows a plot of the average seizure frequency ($\pm$SE) in the four *Scn8a*^{8J} genotypes. The average seizure frequency per hour ($\pm$SE) are: $G_3\times$ C3HeB/FeJ: 132.1 $\pm$ 15.4 (het), 22.3 $\pm$ 4.3 (wt); G_3N_2 and G_3N_3: 104.6 $\pm$ 14.3 (het); (G_3N_3 X C57BL/6J)F1: 80.2 $\pm$ 12 (het), 0.8 $\pm$ .5 (wt); F_1 X C57BL/6J: 60.6 $\pm$ 7.8 (het); C3HeB/FeJ–*Scn8a*$^{med/+}$ 67.9 $\pm$ 2.5.

exhibited 4–5 Hz SWD, slower than those in *Scn8a*^{8J} heterozygotes and most other rodent genetic models and closer to the 3–4 Hz burst frequency of human absence epilepsy. For example, a GEFS+ family with a *GABRG2* R43Q substitution has 3–4 Hz SWD, but the corresponding mutant mice exhibit 7–9 Hz SWD that are typical of other rodent models (28). Our data demonstrate that factors in addition to species differences can influence SWD burst frequency.

Although the behavior of *Scn8a* heterozygous mutants is outwardly normal, systematic testing recently revealed behavioral abnormalities in mice heterozygous for a null allele of *Scn8a* on the C57BL/6J strain background (13). The null heterozygotes exhibited exaggerated conditioned fear, more pronounced avoidance of well-lit environments, and increased response to stress. The direction of the reported effects was consistent with the intermittent cessation of locomotor activity seen during SWD, but in control assays, the heterozygous mice did not differ from wild-type littermates with regard to locomotor activity in a familiar home cage, freezing prior to footshock or performance on the rotorod. As a direct test of the coincidence of behavioral abnormalities with absence seizures, EEG monitoring could be coupled with behavioral tasks in future studies of heterozygous null mice.

Rodent sleep architecture is defined by three different states of vigilance that are influenced by the environment. Sixty to seventy percent of the 12 h light cycle is composed of sleep, which is constantly fragmented by quiet wakefulness. During the 12 h dark cycle, rodents show large periods of active wakefulness that are interrupted by short periods of sleep. In humans and rodents with absence epilepsy, SWD show variable incidence depending on the levels of alertness associated with different states of vigilance (34). EEG analysis during a 48 h period showed that the incidence of SWD during wakefulness in *Scn8a*$^{med/+}$ mutants was not statistically different between light and dark cycles. However, the frequency of SWD during SWS and PS was higher during the dark cycle when compared with the light cycle. During the dark cycle rodents experience light, highly fragmented sleep that facilitates SWD generation (35). In contrast, during the light cycle, mice experience longer periods of consolidated sleep, which is less likely to favor the generation of SWD (35).

An unexpected finding of this study was the observation of a relatively high incidence of SWD during PS. PS is characterized by a desynchronized EEG pattern, which tends to suppress spike-wave activity (36). Less than 20% of SWD in the WAG/Rij rat model of absence epilepsy occurs during PS (34). A recent study conducted in A/J mice demonstrated that only one out of a total of 13 mice exhibited SWD during PS (17). In contrast, we observed SWD in all *Scn8a*$^{med/+}$ mutants during periods of PS. Furthermore, during the 48 h interval the percentage of time spent in

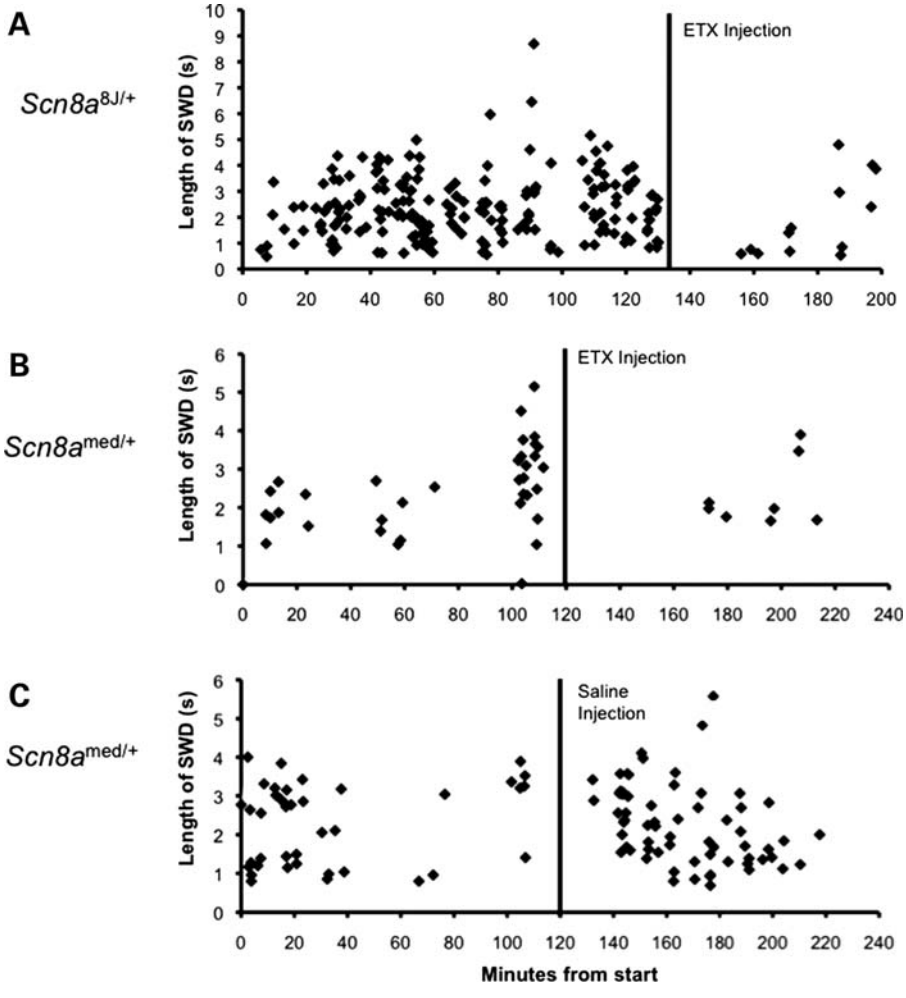

Figure 4. Effect of ETX treatment on SWD in *Scn8a* mutants. ETX treatment decreased the length and incidence of SWD. (**A**) *Scn8a*$^{8J/+}$ examined at Jackson Laboratory. (**B**) *Scn8a*$^{med/+}$ tested at Emory University. (**C**) Effect of the injection procedure on the incidence of SWD. Each diamond represents a single spike-wave discharge, and all of the SWD for a single mouse are shown in each panel. SWD were decreased following ETX administration and increased by the handling associated with saline injection. The average incidence before and after treatment as well as sample sizes are given in Results.

SWD was comparable during wakefulness [0.7% ($\pm$0.2 SE)] and PS [0.6% ($\pm$0.1 SE)] ($P = 0.7$). This suggests that *Scn8a* dysfunction may alter the characteristics (e.g. waveform frequency) of PS. Additional studies will be required in order to more fully characterize the relationship between *Scn8a* dysfunction, sleep architecture and SWD.

In contrast to the higher incidence of absence seizures described above, *Scn8a*^{med} and *Scn8a*$^{med\text{-}jo}$ heterozygotes exhibit increased thresholds for chemically induced convulsive seizures, and the *Scn8a*$^{med\text{-}jo}$ allele can rescue the low seizure threshold of heterozygous *Scn1a* knockout mice (37). Heterozygous *Scn8a* null mutants are also resistant to the initiation and development of kindling (38). This difference may be related to the involvement of different neuronal circuits in absence seizures (thalamocortical circuits) when compared with convulsive seizures. The cellular effect of sodium channel mutations varies in different populations of neurons and may be influenced by the overall channel composition of each neuronal type and by the timing characteristics of the circuit. For example, heterozygosity for a null allele of *Scn1a* has been shown to have a greater effect on bipolar inhibitory neurons of the hippocampus than on pyramidal neurons (39). Similarly, the pain-associated mutation L858H in $Na_v1.7$ renders sensory neurons hyperexcitable and sympathetic neurons hypoexcitable (40).

The WAG/Rij rat strain exhibits a polygenic susceptibility to SWD. In these animals, *Scn8a* ($Na_v1.6$) expression is upregulated in the somatosensory region of the cerebral cortex where SWD are initiated, but it is not clear whether this is a cause or a secondary consequence of the chronic seizure disorder (41). Independently, in a different rat model of absence epilepsy, GAERS, this cortical area was found to be sensitive to the suppression of SWD by local delivery of ETX (42). Since persistent sodium currents have been associated with neuronal burst firing, it could be suggested that overexpression of *Scn8a* could lead to excessive firing in cortical neurons, leading to hyperstimulation of the thalamic portion of the circuit as modeled previously (43). Our results indicate that reduced expression of *Scn8a* contributes to absence epilepsy, because heterozygosity for the null *Scn8a*^{med} allele leads to SWD. The observed epileptogenic effects of both increased and decreased *Scn8a* may be accounted for by

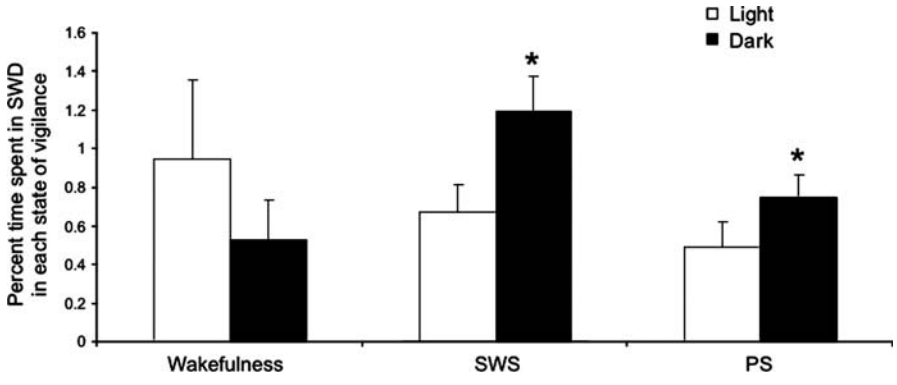

Figure 5. Relationship between SWD and states of vigilance in *Scn8a*$^{med/+}$ mice. The percentage of time spent in SWD during wakefulness was similar in the light and dark cycles. A greater amount of time was spent in SWD during slow-wave sleep (SWS) and paradoxical sleep (PS) in the dark cycle when compared with the light cycle. The percentage of time spent in SWD during wakefulness, SWS and PS was compared between the light and dark cycles using the Wilcoxon signed-rank test implemented in SAS software. *, statistical difference between percentage time spent in SWD in light and dark cycles.

differences among neurons and synapses. For example, reduced *Scn8a* activity may directly increase burst firing of thalamic relay neurons, as suggested for other excitatory neurons, or enhance activity of inhibitory neurons of the reticular thalamic nucleus in a manner suggested for GluR4 mutant mice with SWD (18), producing prolonged inhibition and affect the timing of the thalamocortical oscillation. Further studies of $Na_v1.6$ expression and function in thalamocortical areas will be necessary to reveal more about the pathophysiology of the SWD phenotype in *Scn8a* mutant mice.

The effect of genetic background on absence seizures in heterozygous mice offers a promising model for human absence epilepsy, which is likely to be inherited as a complex trait with dominant allelic behavior. In a human family with a *SCN8A* null allele, heterozygous carriers exhibited variable symptoms, including ataxia and cognitive impairment (14). This family did not undergo EEG analysis, but it is tempting to speculate that abnormal electrical discharges might contribute to their cognitive and behavioral abnormalities. Mutation screening in families with childhood or juvenile absence epilepsy would help evaluate the role of *SCN8A* in human absence epilepsy.

MATERIALS AND METHODS

Mice

The pedigree 596-16 carrying the *Scn8a*^{8J} mutation was obtained from Jackson Laboratory's Reproductive Mutagenesis Program. C3HeB/FeJ (FeJ), C57BL/6J, C3HeB/FeJ-*Scn8a*^{med}/J (Stock no. 003798) and C57BL/6J-*Scn8a*$^{med\text{-}jo}$/J (Stock no. 003799) mice were originally obtained from Jackson Laboratory. All mice were housed in pathogen-free mouse facilities with a 12 h light/dark cycle. Food and water were available *ad libitum*. The Institutional Animal Care and Use Committees (IACUC) at Jackson Laboratory and Emory University approved all experimental protocols involving mice.

Genetic mapping

Genomic DNA from *Scn8a*^{8J} mice was prepared from tail biopsies and initially genotyped by Jackson Laboratory's Genetic Fine Mapping Service using microsatellite markers. For generating the map position, data from telomeric chromosome 15 markers for G_3 and G_3F_1 mice were combined, and the association between genotype and phenotype was tested using the computer program MAPMAKER/QTL. Affected mice were given a value of one and unaffected mice a value of zero. The physical chromosomal coordinates of each marker used to obtain the LOD score plot are shown in Figure 1.

Genotyping assays

The ENU-induced mutation *Scn8a*^{8J} causes loss of a *Bbs*I restriction site in exon 13. The *Scn8a*^{8J} mutation was genotyped by amplification of a 258 bp genomic fragment using the primers 8J-F (5′ GGCCATCATTGTCTTCATCTTTGC) and 8J-R (5′ GAGAAGAAGACGTTGGTACTAACC). Digestion of the PCR product with *Bbs*I generated two 129 bp fragments from the wild-type allele and a single 258 bp fragment from the *Scn8a*^{8J} allele. PCR of genomic DNA was carried out in a 25 μl volume containing 1× GoTaq DNA polymerase buffer (Promega), 2.5 mM $MgCl_2$, 0.2 mM dNTPs, 0.5 M primers and 1 U GoTaq DNA polymerase (Promega). Incubation at 94°C for 2 min was followed by 34 cycles of 94°C for 45 s, 60°C for 45 s and 72°C for 45 s, followed by 72°C for 10 min. Restriction enzyme–digested PCR products were separated on 2% agarose gels and stained with ethidium bromide.

Scn8a$^{med/+}$ mice were genotyped as instructed by Jackson Laboratory (http://jaxmice.jax.org/pub-cgi/protocols/protocols.sh?objtype=protocol&protocol_id=454). Genotyping of the *Scn8a*$^{med\text{-}jo/+}$ mutant was performed using primer pair 8aF (5′ ATGCCACAGAAGTGTCATTCC) and 8aR (5′ GGTATTT CCCAGCAAACAGGT) (32). PCR amplification was performed with one cycle at 94°C for 2 min and 40 cycles of 94°C for 30 s, 55°C for 30 s and 72°C for 1 min. The 213 bp PCR product was digested with *Msl*I to produce fragments of 129, 75 and 9 bp from the wild-type allele, and 102, 75, 27 and 9 bp from the mutant allele.

Mutation detection

The exons and intron/exon boundaries of *Scn8a* were amplified from brain cDNA and genomic DNA prepared from

affected 596-16 mice. Gel-purified PCR products were subjected to automated sequencing in the University of Michigan Sequencing Core.

Western blot

The membrane fraction was prepared from brain homogenates by centrifugation at 100 000*g* as previously described (44). Western blots loaded with 75 μg of membrane protein were hybridized with anti-$Na_v1.6$ antiserum (1:200) from Sigma (S0438, lot 076K1101) as described (45).

EEG analysis

At Jackson Laboratory, *Scn8a*^{8J} mutants 2 months of age or older were anesthetized with tribromoethanol (Avertin, 400 mg/kg i.p.). Small burr holes were drilled (1 mm anterior to bregma and 2 mm posterior to bregma) on both sides of the skull 2 mm lateral to the midline. EEG activity was measured by four Teflon-coated silver wires soldered onto a microconnector. The wires were placed between the dura and the brain and a dental cap was then applied. The mice were given a post-operative analgesic of carprofen (5 mg/kg subcutaneous) and a recovery period of at least 48 h before recordings. The mice were recorded for a 2 h period on two successive days using the Stellate Harmonie headbox, amplifier and software (Stellate, Inc.). SWD, the electroencephalographic feature of absence epilepsy, were defined by a rhythmic oscillation with a burst frequency of 7–9 Hz lasting at least 0.5 s, $>2\times$ background activity, observed in at least two of the six channels. For ETX treatment, on the day following their second standard EEG recording, mice were recorded for 90 min and then injected interperitoneally with 200 mg/kg of ETX (Sigma-Aldrich, Inc.). They were then recorded for a minimum of one additional hour.

At Emory University, 3- to 4-month-old *Scn8a*$^{med/+}$ and *Scn8a*$^{med\text{-}jo/+}$ male mice under deep isoflurane anesthesia were surgically implanted subdurally with four sterile 0-80x3/32 screw electrodes for EEG analysis. Two electrodes were placed on the right hemisphere above the frontal and parietal cortex (2 mm anterior to bregma and 1.2 mm lateral to the midline; and 1.5 mm posterior to bregma and 1.2 mm lateral to the midline, respectively). Contralaterally, the other two electrodes were placed on the left hemisphere above the parietal and visual cortex (0.5 mm posterior to bregma and 2.2 mm lateral to the midline; and 3.5 mm posterior to bregma and 2.2 mm lateral to the midline, respectively). Fine-wire electrodes were inserted into the left and right neck muscles for EMG acquisition. The animals were allowed to recover from surgery for 7 days. Amplified EEG and EMG signals and real-time video signals were collected and processed by Somnologica (Embla Medical, Reykjavik, Iceland) and Stellate Harmonie headbox, amplifier and software (version 6.1, Stellate, Inc.). Baseline EEG activity was recorded for 48 h in *Scn8a*$^{med/+}$ mutants to evaluate the relationship between SWD and different states of vigilance. Each 10 s EEG episode was classified into three different states: wakefulness, SWS and PS. Wakefulness was defined as a low-voltage, high-frequency EEG with elevated and variable EMG. During SWS, the EEG signal increased in amplitude and decreased in frequency with the clear presence of high-amplitude delta waves (0.5–4 Hz), and the EMG signal displayed low regular muscular tone. PS was defined by the presence of regular theta waves (4.5–8 Hz) with lack of muscle tone with phasic bursts of varying duration and amplitude. Following 48 h of sleep/wake analysis, the same data were reanalyzed for number of SWD. SWD were defined by a rhythmic oscillation with a burst frequency of 7–9 Hz lasting at least 0.5 s, $>2\times$ background activity, observed in at least one channel. For each animal, the number of SWD observed in each state of vigilance during the light and dark cycles was divided by the total amount of time spent in each state of vigilance. For ETX treatment, the animals were first injected with saline solution (i.p., 10 ml/kg) to determine whether the handling and injection would alter the number of SWD. Then 48 h later the same animals were injected with ETX (i.p., 200 mg/kg, Sigma-Aldrich, Inc.). The number of SWD was quantified 60 min prior to injection and 60 min following injection of either saline or ETX.

SUPPLEMENTARY MATERIAL

Supplementary Material is available at *HMG* online.

ACKNOWLEDGEMENTS

We thank Dr Zhong-wei Zhang and Dr Greg Cox for critical reading of the manuscript, Carolyne Dunbar and Jonette Gilley for technical assistance and Cheryl Strauss for editorial assistance. We are grateful to Janice Pendola of the Reproductive Mutagenesis Program (supported by NIH grant HD42137) and the Genetic Fine Mapping Service at The Jackson Laboratory for their cited contributions to this work. We thank Dr Allan Levey, Dr David Rye and Dr Glenda Keating for facilitating the experiments conducted in Woodruff Memorial Research Building, Emory University.

Conflict of Interest statement. None declared.

FUNDING

Funding for the study was provided by NIH grants to W.N.F. (NS31348), V.A.L. (NS32801), M.H.M. (NS34509) and A.E. (NS046484). L.P. was supported by fellowships from AFIP and FAPESP (#07/50534-0). S.T. was supported by FAPESP (CEPID#98/14303-3).

REFERENCES

1. Meisler, M.H. and Kearney, J.A. (2005) Sodium channel mutations in epilepsy and other neurological disorders. *J. Clin. Invest.*, **115**, 2010–2017.
2. Kearney, J.A. and Meisler, M.H. *Encyclopedia of Basic Epilepsy Research*, Elsevier. (in press).
3. Holland, K.D., Kearney, J.A., Glauser, T.A., Buck, G., Keddache, M., Blankston, J.R., Glaaser, I.W., Kass, R.S. and Meisler, M.H. (2008) Mutation of sodium channel SCN3A in a patient with cryptogenic pediatric partial epilepsy. *Neurosci. Lett.*, **433**, 65–70.
4. Meisler, M.H., Plummer, N.W., Burgess, D.L., Buchner, D.A. and Sprunger, L.K. (2004) Allelic mutations of the sodium channel SCN8A reveal multiple cellular and physiological functions. *Genetica*, **122**, 37–45.

5. Raman, I.M., Sprunger, L.K., Meisler, M.H. and Bean, B.P. (1997) Altered subthreshold sodium currents and disrupted firing patterns in Purkinje neurons of Scn8a mutant mice. *Neuron*, **19**, 881–891.
6. Maurice, N., Tkatch, T., Meisler, M., Sprunger, L.K. and Surmeier, D.J. (2001) D1/D5 dopamine receptor activation differentially modulates rapidly inactivating and persistent sodium currents in prefrontal cortex pyramidal neurons. *J. Neurosci.*, **21**, 2268–2277.
7. Do, M.T. and Bean, B.P. (2004) Sodium currents in subthalamic nucleus neurons from Nav1.6-null mice. *J. Neurophysiol.*, **92**, 726–733.
8. Cummins, T.R., Dib-Hajj, S.D., Herzog, R.I. and Waxman, S.G. (2005) Nav1.6 channels generate resurgent sodium currents in spinal sensory neurons. *FEBS Lett.*, **579**, 2166–2170.
9. Van Wart, A. and Matthews, G. (2006) Impaired firing and cell-specific compensation in neurons lacking Nav1.6 sodium channels. *J. Neurosci.*, **26**, 7172–7180.
10. Caldwell, J.H., Schaller, K.L., Lasher, R.S., Peles, E. and Levinson, S.R. (2000) Sodium channel Nav1.6 is localized at nodes of Ranvier, dentrites, and synapses. *Proc. Natl Acad. Sci., USA*, **97**, 5616–5620.
11. Van Mart, A., Trimmer, J.S. and Matthews, G. (2007) Polarized distribution of ion channel within microdomains of the axon initial segment. *J. Comp. Neurol.*, **500**, 339–352.
12. Levin, S.I., Khaliq, Z.M., Aman, T.K., Grieco, T.M., Kearney, J.A., Raman, I.M. and Meisler, M.H. (2006) Impaired motor function in mice with cell-specific knockout of sodium channel Scn8a (Nav1.6) in cerebellar purkinje neurons and granule cells. *J. Neurophysiol.*, **96**, 785–793.
13. McKinney, B.C., Chow, C.Y., Meisler, M.H. and Murphy, G.G. (2008) Exaggerated emotional behavior in mice heterozygous null for the sodium channel Scn8a (Nav1.6). *Genes Brain Behav.*, **7**, 629–638.
14. Trudeau, M.M., Dalton, J.C., Day, J.W., Ranum, L.P. and Meisler, M.H. (2006) Heterozygosity for a protein truncation mutation of sodium channel *SCN8A* in a patient with cerebellar atrophy, ataxia, and mental retardation. *J. Med. Genet.*, **43**, 527–530.
15. Gauguier, D., van Luijtelaar, G., Bihoreau, M.T., Wilder, S.P., Godfrey, R.F., Vossen, J., Coenen, A. and Cox, R.D. (2004) Chromosomal mapping of genetic loci controlling absence epilepsy phenotypes in the WAG/Rij rat. *Epilepsia*, **45**, 908–915.
16. Rudolf, G., Bihoreau, M.T., Godfrey, R.F., Wilder, S.P., Cox, R.D., Lathrop, M., Marescaux, C. and Gauguier, D. (2004) Polygenic control of idiopathic generalized epilepsy phenotypes in the genetic absence rats from Strasbourg (GAERS). *Epilepsia*, **45**, 301–308.
17. Strohl, K.P., Gallaugher, L., Lynn, A., Friedman, L., Hill, A., Singer, J.B., Lander, E.S. and Nadeau, J. (2007) Sleep-related epilepsy in the A/J mouse. *Sleep*, **30**, 169–176.
18. Beyer, B., Deleuze, C., Letts, V.A., Mahaffey, C.L., Boumil, R.M., Lew, T.A., Huguenard, J.R. and Frankel, W.N. (2008) Absence seizures in C3H/HeJ and knockout mice caused by mutation of the AMPA receptor subunit Gria4. *Hum. Mol. Genet.*, **17**, 1738–1749.
19. Barclay, J., Balaguero, N., Mione, M., Ackerman, S.L., Letts, V.A., Brodbeck, J., Canti, C., Meir, A., Page, K.M., Kusumi, K. *et al.* (2001) Ducky mouse phenotype of epilepsy and ataxia is associated with mutations in the *Cacna2d2* gene and decreased calcium channel current in cerebellar Purkinje cells. *J. Neurosci.*, **21**, 6095–6104.
20. Burgess, D.L., Jones, J.M., Meisler, M.H. and Noebels, J.L. (1997) Mutation of the Ca^{2+} channel b subunit gene *Cchb4* is associated with ataxia and seizures in the lethargic (*lh*) mouse. *Cell*, **88**, 385–392.
21. Fletcher, C.F., Lutz, C.M., O'sullivan, T.N., Shaughnessy, J.D. Jr, Hawkes, R., Frankel, W.N., Copeland, N.G. and Jenkins, N.A. (1996) Absence epilepsy in tottering mutant mice is associated with calcium channel defects. *Cell*, **87**, 607–617.
22. Letts, V.A., Felix, R., Biddlecome, G.H., Arikkath, J., Mahaffey, C.L., Valenzuela, A., Bartlett, F.S. II, Mori, Y., Campbell, K.P. and Frankel, W.N. (1998) The mouse stargazer gene encodes a neuronal Ca^{2+} channel gamma subunit. *Nat. Genet.*, **19**, 340–347.
23. Ludwig, A., Budde, T., Stieber, J., Moosmang, S., Wahl, C., Holthoff, K., Langebartels, A., Wotjak, C., Munsch, T., Zong, X. *et al.* (2003) Absence epilepsy and sinus dysrhythmia in mice lacking the pacemaker channel HCN2. *EMBO. J.*, **22**, 216–224.
24. Kim, D., Song, I., Keum, S., Lee, T., Jeong, M.J., Kim, S.S., McEnery, M.W. and Shin, H.S. (2001) Lack of the burst firing of thalamocortical relay neurons and resistance to absence seizures in mice lacking $alpha_{1G}$ T-type Ca^{2+} channels. *Neuron*, **31**, 35–45.
25. Singh, B., Monteil, A., Bidaud, I., Sugimoto, Y., Suzuki, T., Hamano, S., Oguni, H., Osawa, M., Alonso, M.E., Delgado-Escueta, A.V. *et al.* (2007) Mutational analysis of CACNA1G in idiopathic generalized epilepsy. Mutation in brief #962. Online. *Hum. Mutat.*, **28**, 524–525.
26. Powell, K.L., Cain, S.M., Ng, C., Sirdesai, S., David, L.S., Kyi, M., Garcia, E., Tyson, J.R., Reid, C.A., Bahlo, M. *et al.* (2009) A $Ca_v3.2$ T-type calcium channel point mutation has splice-variant-specific effects on function and segregates with seizures expression in a polygenic rat model of absence epilepsy. *Neurobiol. Dis.*, **29**, 371–380.
27. Wallace, R.H., Marini, C., Petrou, S., Harkin, L.A., Bowser, D.N., Panchal, R.G., Williams, D.A., Sutherland, G.R., Mulley, J.C., Scheffer, I.E. *et al.* (2001) Mutant GABAA receptor γ2-subunit in childhood absence epilepsy and febrile seizures. *Nat. Genet.*, **28**, 49–52.
28. Tan, H.O., Reid, C.A., Single, F.N., Davies, P.J., Chiu, C., Murphy, S., Clarke, A.L., Dibbens, L., Krestel, H., Mulley, J.C. *et al.* (2007) Reduced cortical inhibition in a mouse model of familial childhood absence epilepsy. *Proc. Natl Acad. Sci., USA*, **104**, 17536–17541.
29. Kohrman, D.C., Harris, J.B. and Meisler, M.H. (1996) Mutation detection in the *med* and *med^J* alleles of the sodium channel *Scn8a*. *J. Biol. Chem.*, **271**, 17576–17581.
30. Buchner, D.A., Seburn, K.L., Frankel, W.N. and Meisler, M.H. (2004) Three ENU-induced neurological mutations in the pore loop of sodium channel Scn8a (Na(v)1.6) and a genetically linked retinal mutation, rd13. *Mamm. Genome*, **15**, 344–351.
31. Frankel, W.N., Beyer, B., Maxwell, C.R., Pretel, S., Letts, V.A. and Siegel, S.J. (2005) Development of a new genetic model for absence epilepsy: spike-wave seizures in C3H/He and backcross mice. *J. Neurosci.*, **25**, 3452–3458.
32. Kohrman, D.C., Smith, M.R., Goldin, A.L., Harris, J. and Meisler, M.H. (1996) A missense mutation in the sodium channel Scn8a is responsible for cerebellar ataxia in the mouse mutant jolting. *J. Neurosci.*, **16**, 5993–5999.
33. Glauser, T.A., Morita, D.A. and Wyllie, E. (eds) (2006) *The Treatment of Epilepsy, Principles and Practice*, Lippincott Williams & Wilkins, Philadelphia, PA.
34. Drinkenburg, W.H., Coenen, A.M., Vossen, J.M. and van Luijtelaar, E.L. (1991) Spike-wake discharges and sleep-wake state in rats with absence epilepsy. *Epilepsy Res.*, **9**, 218–224.
35. Coenen, A.M. and van Luijtelaar, E.L. (2003) Genetic animal models for absence epilepsy: a review of the WAG/Rij strain of rats. *Behav. Genet.*, **33**, 635–655.
36. Coenen, A.M., Drinkenburg, W.H., Peeters, B.W., Vossen, J.M. and van Luijtelaar, E.L. (1991) Absence epilepsy and the level of vigilance in rats of the WAG/Rij strain. *Neurosci. Biobehav. Rev.*, **15**, 259–263.
37. Martin, M.S., Tang, B., Papale, L.A., Yu, F.H., Catterall, W.A. and Escayg, A. (2007) The voltage-gated sodium channel *Scn8a* is a genetic modifier of severe myoclonic epilepsy of infancy. *Hum. Mol. Genet.*, **16**, 2892–2899.
38. Blumenfeld, H., Lampert, A., Klein, J.P., Mission, J., Chen, M.C., Rivera, M., Dib-Hajj, S., Brennan, A.R., Hains, B.C. and Waxman, S.G. (2009) Role of hippocampal sodium channel Nav1.6 in kindling epileptogenesis. *Epilepsia*, **50**, 44–55.
39. Yu, F.H., Mantegazza, M., Westenbroek, R.E., Robbins, C.A., Kalume, F., Burton, K.A., Spain, W.J., McKnight, G.S., Scheuer, T. and Catterall, W.A. (2006) Reduced sodium current in GABAergic interneurons in a mouse model of severe myoclonic epilepsy in infancy. *Nat. Neurosci.*, **9**, 1142–1149.
40. Rush, A.M., Dib-Hajj, S.D., Liu, S., Cummins, T.R., Black, J.A. and Waxman, S.G. (2006) A single sodium channel mutation produces hyper- or hypoexcitability in different types of neurons. *Proc. Natl Acad. Sci. USA*, **103**, 8245–8250.
41. Klein, J.P., Khera, D.S., Nersesyan, H., Kimchi, E.Y., Waxman, S.G. and Blumenfeld, H. (2004) Dysregulation of sodium channel expression in cortical neurons in a rodent model of absence epilepsy. *Brain Res.*, **1000**, 102–109.
42. Manning, J.P., Richards, D.A., Leresche, N., Crunelli, V. and Bowery, N.G. (2004) Cortical-area specific block of genetically determined absence seizures by ethosuximide. *Neuroscience*, **123**, 5–9.
43. Blumenfeld, H. and McCormick, D.A. (2000) Corticothalamic inputs control the pattern of activity generated in thalamocortical networks. *J. Neurosci.*, **20**, 5153–5162.
44. West, J.W., Scheuer, T., Maechler, L. and Catterall, W.A. (1992) Efficient expression of rat brain type IIA Na+ channel alpha subunits in a somatic cell line. *Neuron*, **8**, 59–70.
45. Levin, S.I. and Meisler, M.H. (2004) Floxed allele for conditional inactivation of the voltage-gated sodium channel Scn8a ($Na_v1.6$). *Genesis*, **39**, 234–239.